Available online at www.sciencedirect.com
SCIENCE DIRECT®
International Journal of Heat and Mass Transfer 48 (2005) 2299–2309
International Journal of HEAT and MASS TRANSFER
www.elsevier.com/locate/ijhmt

Apparatus for investigation of evaporation at free liquid–vapour interfaces

S. Popov [a], A. Melling [a], F. Durst [a,*], C.A. Ward [a,b]

[a] Institute of Fluid Mechanics, University of Erlangen-Nürnberg, Cauerstrasse 4, D-91058 Erlangen, Germany
[b] Department of Mechanical and Industrial Engineering, University of Toronto, Toronto, Ont., Canada M5S 3G8

Received 21 November 2003; received in revised form 16 September 2004
Available online 17 March 2005

Abstract

Experimental data for the evaporation coefficients of water have indicated a scatter over four orders of magnitude. One source of uncertainty in the data is probably the temperature at the liquid–vapour interface; recently published results in an axisymmetric geometry show temperature jumps of several °C at the free surface of evaporating water, contradicting the established assumption of a unique temperature in the liquid and vapour phases at the interface. In an apparatus with a two-dimensional geometry, temperature profiles in both phases near the interface during steady state evaporation confirm the earlier measurements and indicate the suitability of the apparatus for measurements close to the interface.

1. Introduction

Recent studies of liquid evaporation have raised questions about the conditions existing at the interface of an evaporating liquid, and indicated strong disagreement between theory and experiment. Of most concern, even the experimental results reported from different laboratories have not been consistently interpreted.

1.1. Theoretical work

Several theoretical approaches have been used to examine the interfacial conditions during evaporation. The Stefan condition [18,19] assumes that thermal conduction in the liquid and vapour phases supplies the energy to the interface where the phase change takes place. No assumption is made on the value of the interfacial temperatures, but the temperature gradients in each phase are assumed to be sufficiently large to supply the required energy.

This approach neglects thermocapillary convection, but careful measurements of the temperature profiles in the liquid and vapour phases of water during steady-state evaporation indicate that thermal conduction only accounts for about 50% of the energy transport required to evaporate the liquid at the observed rate [21]. In order to have an energy balance, the thermocapillary convection would have to supply the remainder of the energy. Also, a uniform temperature layer was measured immediately below the water–vapour interface and it was suggested [24] that this may have come from the mixing produced by the thermocapillary convection. The thickness of this layer varied with the evaporation rate, but was on the order of 0.5 mm.

* Corresponding author. Tel.: +49 9131 85 29501; fax: +49 9131 85 29503.
E-mail address: durst@lstm.uni-erlangen.de (F. Durst).

0017-9310/$ - see front matter © 2005 Elsevier Ltd. All rights reserved.
doi:10.1016/j.ijheatmasstransfer.2004.10.038

Nomenclature

h	specific enthalpy
k	thermal conductivity
K_c	condensation coefficient
K_e	evaporation coefficient
$\dot{m}''$	mass flux
p	pressure
$\dot{q}''$	heat flux
T	temperature
x	Cartesian coordinate
y	Cartesian coordinate
z	Cartesian coordinate

Subscripts

I	interface
c	thermocouple
s	surroundings

Superscripts

L	liquid
V	vapour

Studies based on classical kinetic theory led to the Hertz–Knudsen–Schrage equation [7,16] in which the evaporation flux is expressed in terms of the interfacial temperatures, T_I^V and T_I^L, the interfacial pressures, p_I^V and p_I^L, and the evaporation and condensation coefficients, K_e and K_c. However, this approach has come under question because the evaporation coefficient values reported by different investigators and analyzed by Marek and Straub [11] vary by over four orders of magnitude. Such a wide variation in the empirical values of the evaporation coefficient suggests a substantial difficulty either with the theory or with the measurement of the conditions at the interface.

Although still based on classical kinetic theory, Pao [13,14] advanced an approach in which the evaporation and condensation coefficients were assumed unity, and classical kinetic theory was used to predict the temperature profile between two horizontal liquid films maintained at different temperatures. At one film, evaporation was supposed and at the other condensation. For a liquid such as water it was predicted that at the liquid–vapour interface of the evaporating film the interfacial vapour temperature would be *less* than that of the liquid, and that at the condensing interface the temperature discontinuity would be in the opposite direction. The temperature discontinuities were of sufficient magnitude that the gradient of the temperature in the vapour phase between the liquid layers was predicted to be in the opposite direction to the applied temperature gradient. These *predictions* were confirmed by other *analytical* investigations, including non-equilibrium thermodynamics [1], but some investigators considered such temperature profiles to be non-physical and labelled them "inverted", "anomalous" or "paradoxical" [8]. Others argued strongly in their favour [17].

1.2. Experimental work

Experimental studies have not resolved the controversy, but some published data which appear to support, or at least not contradict, the "anomalous" temperature profiles were obtained with questionable experimental techniques. Shankar and Deshpande [17] measured the temperature distribution near the interface of water evaporating into a vapour–air mixture with thermocouples constructed of approximately 300 μm diameter wire—the size of the bead was not given. They did not record any interfacial temperature discontinuity, nor any evidence of an anomalous temperature profile, but such a large thermocouple would not have allowed measurements to be made very close to the interface. As will be seen, the locations of temperature measurements in each phase relative to the interface is important in determining whether a temperature discontinuity will be detected. Further, their thermocouples were fixed in position, and there was no way they could have precisely measured their position relative to the interface. Finally, it is not clear that the liquid was evaporating under steady state conditions, as assumed in the theory proposed by Pao and others.

Hisatake et al. [6] used a smaller thermocouple, 127 μm diameter, to study the temperature profile near the interface of water as it evaporated into an air–vapour mixture. They were able to get much closer to the interface than were Shankar and Deshpande. The temperature profile they obtained is very similar to that subsequently reported by Ward and co-workers [4,5,12,21,24] but the interpretation was different. The Hisatake et al. measurements indicated a decreasing liquid phase temperature as the thermocouple approached the liquid–vapour interface from within the liquid and then a sudden increase in temperature as the thermocouple entered the vapour phase. They did not interpret the temperature at the interface as being discontinuous, but drew a smooth curve through the measured temperature points, so obtaining a minimum temperature *in the liquid phase* below the interface. Thus, there would have had to be a heat sink in the liquid phase near the interface, but this seems to be a non-physical interpretation.

A still smaller thermocouple (about 25 μm diameter) was used by Fang and Ward [4,5,22] to study evaporation of pure water. This allowed them to get closer to the interface than had any of the previous investigators. In one of their experiments they were able to get their thermocouple in the vapour phase within approximately one mean free path of the interface. Thus the molecules evaporating from the liquid phase encountered the thermocouple at approximately the same time as they underwent their first collision with other vapour molecules. In this experiment, they measured the largest temperature discontinuity; the interfacial vapour temperature was 7.8 °C *greater* than the interfacial liquid temperature [4]. In other studies [5,21,22,24] using three different liquids, each evaporating under steady state conditions, a temperature discontinuity was found at the liquid–vapour interface and the interfacial vapour temperature was again reported to be greater than that in the liquid. The liquid–vapour interface was curved and in most cases evaporated under steady-state conditions. We emphasize that this measured temperature discontinuity was in the opposite direction to that predicted using classical kinetic theory [13,14] and non-equilibrium thermodynamics [1], and it raises questions about the validity of those theoretical approaches when applied to phase change [8].

We note that the measured temperature discontinuity in which the interfacial vapour temperature is greater than that in the liquid is not without theoretical support. Ward and Fang [22] extended statistical rate theory [3,20,23] so it could be applied to predict molecular transport across non-isothermal interfaces between macroscopic phases. This theory may be used to predict the pressure in the vapour phase during evaporation from measured values of instantaneous evaporation flux, interfacial liquid and vapour temperatures and interfacial liquid pressure. The parameters that appear in the expression for vapour phase pressure are the material properties of the substance evaporating, such as the saturation vapour pressure and the surface tension, and certain molecular properties, such as the vibrational frequencies of the molecule and the vibrational partition function. For water all of these parameters have been independently determined, so Ward and Fang [22] were able to compare predictions for water evaporation with the measurements found in 15 experiments over a wide range of evaporation rates. No discrepancy between the measured and predicted values of the vapour phase pressure was found within the experimental uncertainty of ±13 Pa. Recently, Rahimi and Ward [15] used an improved technique for measuring vapour phase pressure during water evaporation from capillaries and reported that the discrepancy between the measured pressure and that predicted from statistical rate theory was no greater than 0.004 Pa.

1.3. Present work

Only investigators studying a curved, axisymmetric liquid–vapour interface have reported an interfacial temperature discontinuity during evaporation [4,5,12,21,22,24]. Those who studied evaporation at an interface with a flat liquid–vapour interface either did not find a temperature discontinuity [17] (perhaps because of the size of the thermocouple used) or did not interpret their measurements as indicating a temperature discontinuity [6]. Since the possible existence of a temperature discontinuity at the liquid–vapour interface in which the temperature in the vapour is greater than that in the liquid raises fundamental questions about classical kinetic theory and non-equilibrium thermodynamics, it seems important to examine the phenomena under different experimental conditions.

Consequently, for the present studies an apparatus was constructed in which water evaporated from the rectangular (8 mm × 22 mm) mouth of a funnel. Both curved and flat liquid–vapour interfaces were examined. A thermocouple made from 25 μm diameter wire was used; a careful welding technique gave a junction of almost the same size as the wire. The thermocouple was mounted on a micro-positioner that allowed its position to be controlled to within ±10 μm. The liquid–vapour interface could be viewed from outside the evaporation chamber and its position measured with a cathetometer. The interface could be maintained at a constant position by supplying liquid at the bottom of the funnel at the same rate as it evaporated. Finally, the entrance to the funnel could be thermostated at a chosen temperature less than 4 °C, where water has its maximum density. Because of the evaporation at the interface, the temperature at the interface was less than that at the entrance to the funnel. The lower temperature water at the interface, therefore, had a lower density so that no buoyancy-driven convection occurred in our experiments [21,24].

Section 2 describes the apparatus which permitted temperature profile measurements both along and perpendicular to the interface. The verification experiments described in Section 3 show temperature profile characteristics in a two-dimensional configuration similar to those found in the axisymmetric configuration of the earlier experiments. Conclusions of the work are summarized in Section 4.

2. Test apparatus and experimental procedure

2.1. Test apparatus

The test rig was based on an earlier facility in Toronto [4], but incorporated a newly designed test cell, Fig. 1. While in the Toronto cell an axisymmetric interface

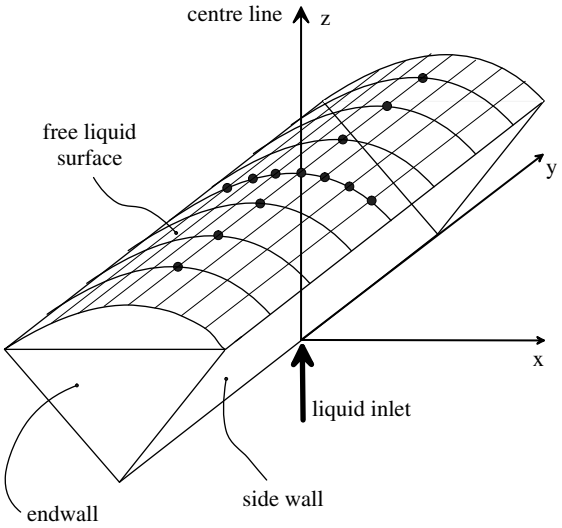

Fig. 1. Test section and location of temperature profiles.

between the liquid and gas phases was created on top of a conical liquid pool, in the present investigations the liquid was contained in a channel-like pool giving a two-dimensional interface. The channel was formed by milling a groove (length 24 mm, included angle 110°, width at the top 8 mm) in a stainless steel block. This block was mounted in a plexiglas tube which in turn was fastened and hermetically sealed with O-rings to two air-tight flanges, so that the apparatus could be evacuated. An opening in the middle of the channel permitted the supply of water through a thin stainless steel tube connected with a microlitre syringe pump. Visual observation of the water surface through the transparent plexiglas tube (internal diameter 42 mm) permitted the water level to be read with a cathetometer. By controlling the feed rate of water and the evaporation rate, the location of the free water surface could be maintained constant throughout an experiment.

The two-dimensional channel geometry was chosen to expand the data base against which the theory [5,22] could be tested. Plane glass windows were inserted into the end walls of the channel, so that the application of optical velocity measuring techniques at a later stage would not be prohibited. The maximum amplitude of the Marangoni velocity generated by water evaporation from the mouth of a circular cone, however, as inferred in a recent study [24] from the deflection of a tiny probe (12.5 μm diameter) and calculated from the measured temperature gradient in the liquid phase, was only 0.75 mm/s. The very small magnitudes of the convection velocities and the high spatial resolution necessary in the vicinity of the liquid–vapour interface pose severe requirements on instrumentation. It is thus expected that velocity measurements would be extremely difficult to obtain either with laser Doppler anemometry or with particle image velocimetry. In the present paper, therefore, attention was directed solely at acquiring temperature data in a two-dimensional geometry to supplement and for comparison with previous results in an axisymmetric geometry.

2.2. Experimental procedure

The following preparations preceded each test series in the apparatus shown in Fig. 2.

- All valves were closed and the measurement cell was evacuated with the turbomolecular pump (TMP) to the lowest pressure achievable with unavoidable leakage through the O-rings (0.22 Pa).
- During the evacuation the water reservoir was filled with fresh highly purified water, the cold trap was filled with liquid nitrogen and the mechanical pump connected to the cold trap was switched on.
- The vacuum valve on the reservoir was then opened. The water began to bubble as dissolved air, responsible for bubble nucleation, escaped from the water. After about 20 min most of the gaseous impurities were removed from the water.
- The vacuum valve was closed and the water was slowly warmed to promote faster degasification than in the water cooled by the intensive evaporation. The cold trap was continuously supplied with liquid nitrogen.
- After reaching a temperature of about 50 °C the vacuum valve was again opened. The water in the glass container was superheated, since very few nucleation centres were present for bubble formation. This led to easily visible explosive processes accompanied by audible crackling. When this condition was reached, the water was fully degasified. About 1/5 of the quantity of water in the reservoir was lost in the cold trap and the rest was available for the measurement.
- The valve to the TMP was then closed to protect the pump from damage due to the water vapour.
- The valve between the glass reservoir and the measurement cell was carefully opened, the syringe was filled with water and the valve was again closed.
- Thereafter nitrogen was let into the measurement cell until the pressure reached 320 kPa. After an hour under the influence of the applied pressure all gaps and pores in the piping between the syringe and the test rig were filled with water and the experiment could begin. The thermostat was allowed to cool to the operating temperature (about 2 °C) and stabilize there.
- The mechanical pump was switched on and the nitrogen was pumped out of the measurement cell. The pressure fell slowly to the desired level for a particular measurement.

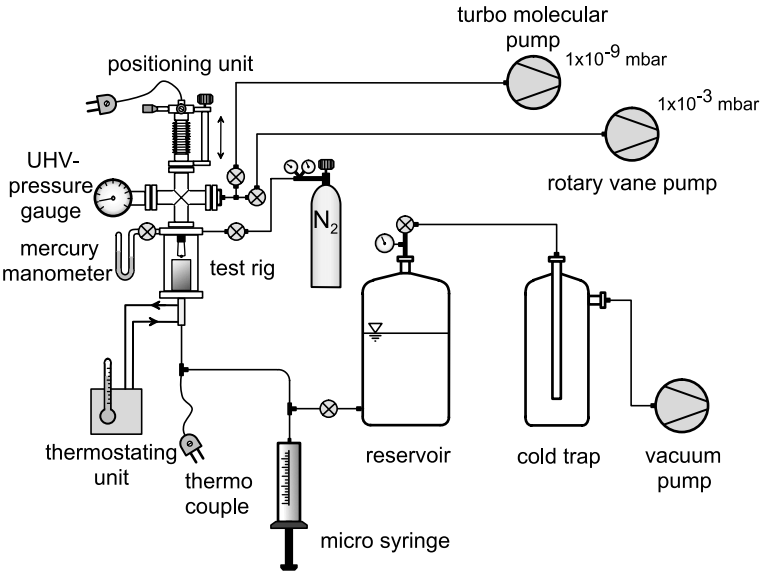

Fig. 2. Test equipment.

- A steady condition was sought by adjustment of the pressure in the measurement cell and the pumping rate of the microlitre syringe pump. After reaching this condition the measurement of a temperature profile could begin.

In each experiment the temperature of the water entering the channel was maintained less than 4 °C. As a result of evaporation the liquid near the liquid–vapour interface was cooled below the temperature of the water entering the channel. Since the density of water decreases with decreasing temperature for temperatures below 4 °C, the less dense liquid was at the liquid–vapour interface. Thus, in these experiments (as in previous experiments [4,21,22,24]) there was no buoyancy-driven convection.

2.3. Temperature measurement

A fine wire thermocouple was chosen for the temperature measurements because of its advantages of good spatial resolution, easy positioning and short response time. The response time in particular was critical to reduce the total measuring time because the duration of each experiment was limited by the quantity of water in the syringe pump.

A type K thermocouple was manufactured by welding 25 μm chromel and alumel wires (Fig. 3). The thermocouple leads were bent so that they would lie along the same temperature level as the weld up to a distance of about 0.5 mm from the weld. This minimized the disturbance due to heat conduction along the thermocouple leads in a strong temperature gradient. The thermocouple was used with a PC measurement electronics of type OMEGA OMB-DAQ-55 from Newport Electronics which contained five differential analog inputs with 22 bit resolution. For voltage measurements a mode with continuous self-calibration was chosen, permitting stable zero-point measurements over 320 s. The "cold" junction was placed in a thermos flask which acted as an ice bath with a stable reference temperature of 0 °C for an extended period.

For calibration, the measuring junction of the thermocouple was immersed in an ethanol/water mixture in a calibration cell. This cell had a double glass wall and was equipped with a thermostat (Haake) covering a temperature range between −40 °C and +120 °C with a temperature stability of ±0.02 K. For the exact temperature measurement in the calibration cell a 1/10-DIN Pt100 temperature probe was used. The calibration curve at six points is shown in Fig. 4. A conversion formula from voltage to temperature was found by linear regression with the program Origin. The standard deviation of the points from a straight line fit was only 0.03 K.

For temperature profile measurements in the gas phase, the thermocouple was first positioned 10 μm above the surface with the help of a cathetometer. Immediately adjacent to the surface the temperature was recorded at six points at intervals of 100 μm. Subsequently measurements were made at five steps with a separation of 200 μm up to a height of 1.5 mm above the phase interface. To minimize the duration of the experiment, further measuring points were taken with spacings of 1 and 2 mm up to 12 mm, giving a temperature profile with 17 measuring points.

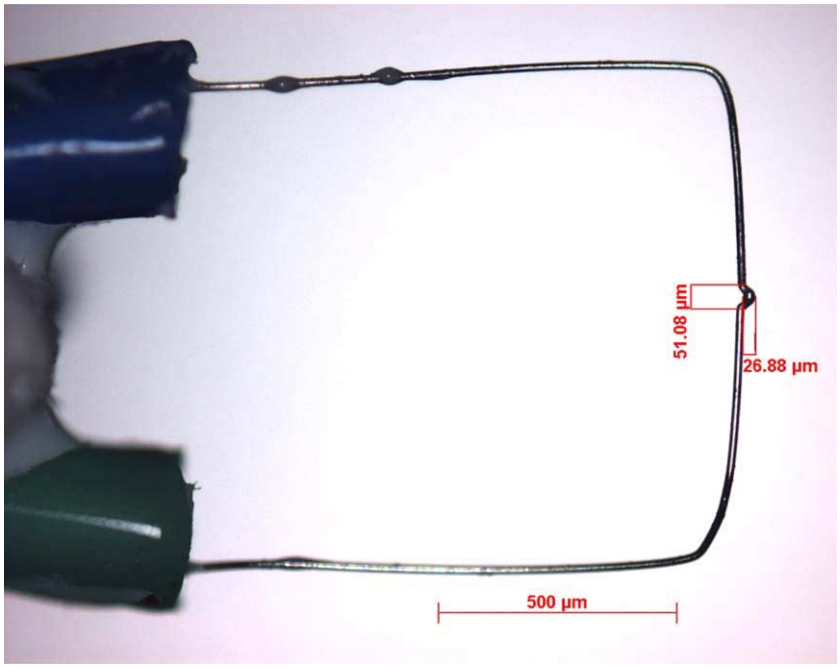

Fig. 3. Thermocouple, 25 µm wire diameter.

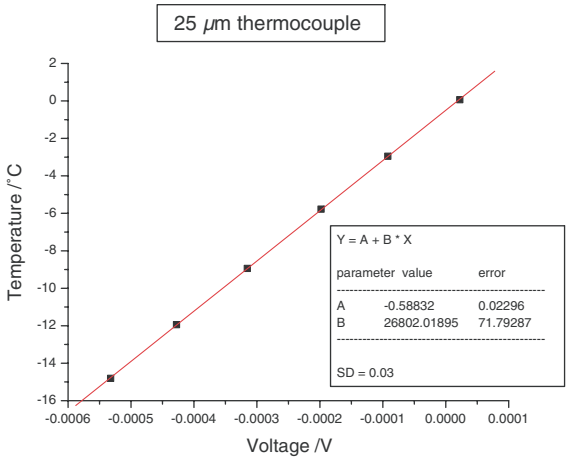

Fig. 4. Calibration curve of type K thermocouple.

Thereafter followed the measurements in the liquid phase. After noting the exact position of the phase interface the thermocouple was moved down until the head overcame the surface tension. Then the thermocouple was moved to the previously noted position to start the measurements. These were made in 50 µm steps down to a depth of 500 µm (11 points) through a layer at initially constant temperature. Then followed steps of 100 µm as far as a depth of 2 mm. Altogether 22 measuring points were taken in the liquid phase. The measuring time for 39 points in both phases was about one hour. At low evaporation rates four to five profiles could be taken with one filling (10 ml) of the water supply syringe. Throughout the measurements the pressure was monitored and adjusted for constancy if necessary.

Temperature profiles were recorded on the centre line, as well as in front of, behind and to the side of the centre line. The black points in Fig. 1 indicate the positions where temperature distributions were determined.

2.4. Measurement uncertainty

In making the temperature measurements there may be concerns about effects of thermal radiation on the temperature jump with a dry or wetted thermocouple junction and the size of the thermocouple relative to the measuring distance from the interface.[1]

The thermocouple was approximately 10 µm from the colder liquid surface when the temperature jump was measured, and the warmer surroundings were about 50 mm (or 5000 times further) away. Thus, the shape factor between the thermocouple and the liquid determined the dominant radiation exchange. Also, the temperature of the thermocouple, T_c, was about 263 K and that of the surroundings, T_s, was say 300 K, indicating a temperature factor $(T_c/T_s)^4 \simeq 0.6$. Thus, the dominant radiation exchange of the thermocouple took place with

[1] The authors are grateful to the reviewers for suggesting that these points be addressed in the paper.

the colder liquid. The temperature of the vapour was, therefore, "warmer" than the temperature read by the thermocouple, so that the measured temperature jump values were very slightly conservative.

When the thermocouple was brought out of the liquid and into the vapour, it was held at a position about 10 μm above the liquid until it reached steady state. The vapour phase was superheated, since the pressure in the vapour was less than the saturation vapour pressure. (For the experiment shown in Fig. 6, for example, the temperature in the vapour was −3.4 °C. The saturation vapour pressure corresponding to this temperature is 475.6 Pa [10] while the measured pressure was 240 Pa.) Thus, any liquid film on the thermocouple would have evaporated when the thermocouple was brought out of the liquid. So the recorded steady-state temperature was the vapour temperature since no liquid film was present.

The temperature uncertainty of the Pt100 resistance thermometer used in the calibration cell was ±0.03 K at 0 °C and ±0.08 K at −10 °C.

3. Temperature distribution measurements near the phase interface

3.1. Preliminary temperature measurements

First measurements of the temperature distribution at the phase interface were used to test the apparatus. The results shown in Figs. 5 and 6 were obtained at different pressures, 240 and 190 Pa, respectively. A linear variation of the temperature distribution in the liquid phase is readily seen, indicative of heat transfer by conduction. A temperature jump at the phase interface is also evident, in the direction reported by Fang and Ward [4]: the temperature in the gas phase is higher than in the liquid phase, so that the lowest measured temperature is found at the highest point in the liquid.

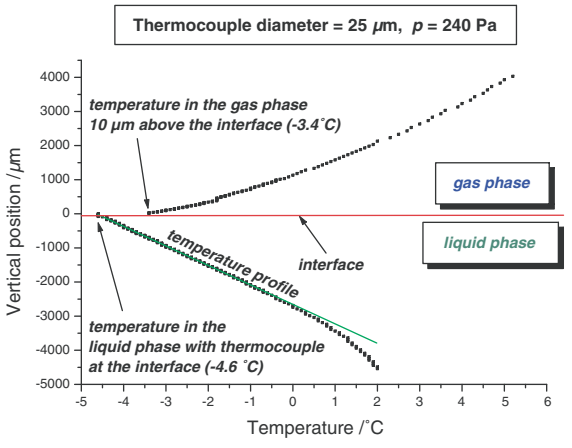

Fig. 5. Temperature profile in preliminary experiments; pressure 240 Pa.

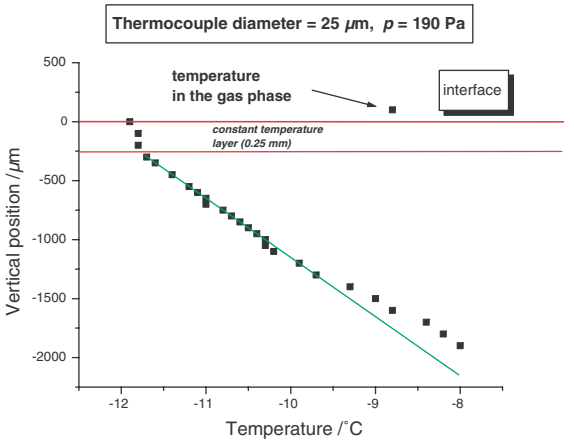

Fig. 6. Temperature profile in preliminary experiments; pressure 190 Pa.

While the temperature jump in Fig. 5 is only 1.2 K, Fig. 6 indicates a temperature jump of 3 K because a lower pressure above the liquid leads to a higher rate of evaporation. Here the constant temperature layer is quite clearly observed. The temperature at the surface decreased with reduced pressure, but according to the vapour pressure curve of water [10] the measured pressure corresponded to a significantly lower temperature than that measured. Unfortunately the electronic pressure gauge was found subsequently to be reading incorrectly, but the trend of the relationship between temperature jump and pressure was uninfluenced by this discrepancy.

According to the procedure described in Section 2.3 for positioning the thermocouple in the liquid phase, this traverse started with the middle point of the thermocouple located at the level M of the undisturbed interface. It is important to note that the measured temperature at this position was nevertheless the liquid temperature and not some undetermined average of the temperatures in the liquid and gas phases, respectively. Position M was identified by a rapid change in the output of the thermocouple as it was brought down to the interface from above, caused by a pronounced change in heat transfer rate as the thermocouple came into contact with the surface of the liquid. With further downward movement of the thermocouple the interface became more and more distorted as surface tension effects initially prevented the thermocouple from breaking through the interface. Temperature measurements were not made under this condition. After overcoming the surface tension the probe was then moved back to the position M. Now, however, the thermocouple surface was fully wetted and the indicated temperature at points marked

on the interface in Fig. 5 and the following figures was the liquid phase temperature.

The temperature distributions in Figs. 5 and 6 indicate temperatures significantly below 0 °C, but the water was still present in liquid form because of the low pressure. For example, at −5 °C water vapour would be in equilibrium with ice at a pressure of 402 Pa [10, p. 6–9]; however, as indicated in Fig. 5, the pressure was only 240 Pa. In the profile indicated in Fig. 6 the temperature approached −12 °C at a pressure of 190 Pa. At this temperature, ice would be expected only if the pressure were greater than 217 Pa.

Susceptibility to influences from small amounts of impurities in the water at the low pressure in our experiments, about 290 Pa, might be expected. The water used, however, had a high purity according to manufacturer's specifications, was transferred directly into a degassing vessel and then after degassing directly into the evaporation chamber without further exposure to air. Thus, the water was initially highly purified and the handling process ensured the minimization of impurities.

These preliminary temperature measurements permitted only qualitative conclusions about the temperature jump and the temperature distribution. Further experiments under improved conditions were therefore carried out to obtain quantitative insight into the phenomena.

3.2. Vertical temperature distributions and two-dimensionality of the temperature field

After detail improvements in the test apparatus more nearly constant conditions could be secured than in the case of the measurements presented in Figs. 5 and 6. A mercury-in-glass U-tube manometer instead of an electronic manometer permitted a significant improvement of the reading of the pressure prevailing in the measuring cell.

A first measurement was made without evaporation. To this end water was introduced into the measuring cell which was evacuated for a short time to allow water droplets which may have accumulated outside the interesting region to evaporate. Then all valves were closed and the water supply was interrupted. Under these conditions the measuring cell was a closed system because no water could reach it from the microlitre syringe and no water vapour could escape. After allowing the measuring cell to reach steady state, the temperature profile presented in Figs. 7 and 8 was recorded. The temperature of the water at the bottom of the channel was maintained at 3.03 ± 0.03 °C and the temperature at the interface was slightly higher, 3.58 ± 0.01 °C. As indicated in Fig. 8, there was a temperature discontinuity at the interface with the interfacial temperature in the vapour greater than that in the liquid by 0.36 °C. The saturation pressure corresponding to the temperature

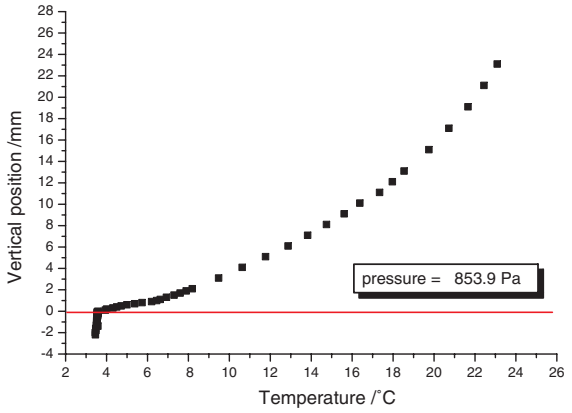

Fig. 7. Temperature profile without evaporation; water temperature at entry = 3.03 ± 0.03 °C.

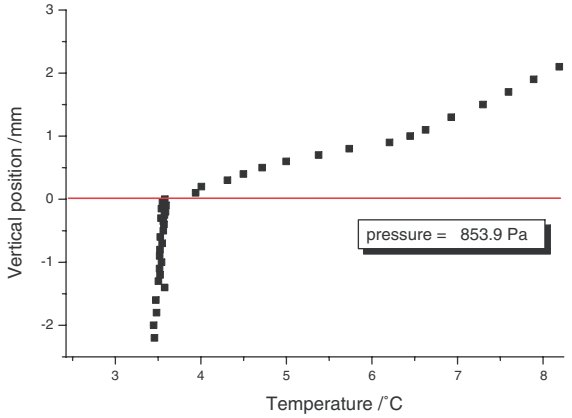

Fig. 8. Temperature profile without evaporation (enlarged); water temperature at entry = 3.03 ± 0.03 °C.

of the liquid at the interface (3.94 °C) was 816.7 Pa and the measured pressure in the vapour was 853.9 Pa. Thus, condensation was taking place at the interface, but the rate of condensation was so small that the interface movement was not measurable.

Ward and Stanga [24] have studied the conditions at the interface of water during condensation. They also observed a temperature discontinuity in which the interfacial temperature in the vapour was greater than that in the liquid. Experiments show that the direction of the interfacial temperature discontinuity is the same for either evaporation or condensation at the interface.

Since no vapour was formed and the rate of condensation was negligible, the transported heat must be the same in both phases ($\dot{q}''^{\mathrm{L}} = \dot{q}''^{\mathrm{V}}$). According to the equation

$$\dot{q}'' = -k\frac{\mathrm{d}T}{\mathrm{d}z} \tag{1}$$

the temperature gradient dT^L/dz in the liquid phase must be smaller than the gradient dT^V/dz in the vapour phase because of the larger thermal conductivity k. The first temperature point in the gas phase was measured at a distance of about 100 μm from the phase interface. By extrapolating the temperature profile in the gas phase in the direction of the phase boundary the unique temperature at the water surface is reached, as expected in the absence of phase change.

For measurements with evaporation, the temperature of the water entering the channel was maintained at -0.26 ± 0.07 °C. The complete temperature profile on the centre line and the conditions existing in the cell are given in Fig. 9. In Fig. 10 an enlarged portion in the region near the phase boundary shows clearly a temperature jump of about 1.2 K as well as a layer of about 0.3 mm thickness with approximately constant temperature.

Using the measured temperature distribution and Eq. (1) to calculate the heat fluxes $\dot{q}''^L$ and $\dot{q}''^V$ in the liquid and vapour phases, respectively, the rate of evaporation $\dot{m}''$ determined with the Stefan equation (2) was 0.817 g m^{-2} s^{-1}:

$$\dot{m}'' = \frac{\dot{q}''^L - \dot{q}''^V}{h^V - h^L} \tag{2}$$

where h is the specific enthalpy. This value is about 3.5 times smaller than the value (2.835 g m^{-2} s^{-1}) for the rate of evaporation determined from the flow rate from the microlitre syringe and the total surface area of the phase boundary. An explanation of this difference is deferred to the discussion in Section 3.3.

Next the temperature distributions in the water were measured and compared along the centre line and at two stations located 6 mm left and 6 mm right of the centre line, i.e., at $x = \pm 6$ mm in Fig. 1. To facilitate the comparison in Fig. 11 the axes have been interchanged with respect to the previous figures. In these experiments the inlet temperature was held fixed as follows: centre -0.21 ± 0.06 °C, left 0.00 ± 0.05 °C, right $+0.05 \pm 0.05$ °C. The temperature distributions left and right of the centre line confirm the expected symmetry in the temperature field according to the geometrical symmetry. Another interesting feature is evident: while the layer of constant temperature along the centre line is very clearly seen, it is not present in the temperature profiles to the side of the centre line.

To clarify the importance of the heat flux on the evaporation, a further set of two measurements was made with different water levels in the channel at a pressure of 284.6 Pa. In the first case the surface was flat, so that at the deepest point of the channel the depth was 3 mm; the overall surface area was fixed by the length and width of the channel. In the second case the maximum depth was 4.5 mm and the surface area was correspondingly greater because of surface curvature. Nevertheless, the rate of evaporation from the flat

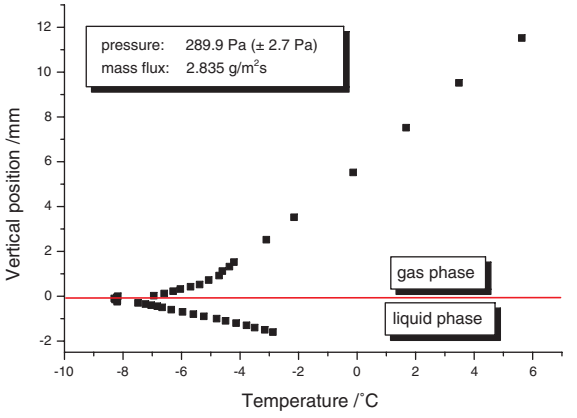

Fig. 9. Temperature profile on the centre line with evaporation; water temperature at entry = -0.26 ± 0.07 °C.

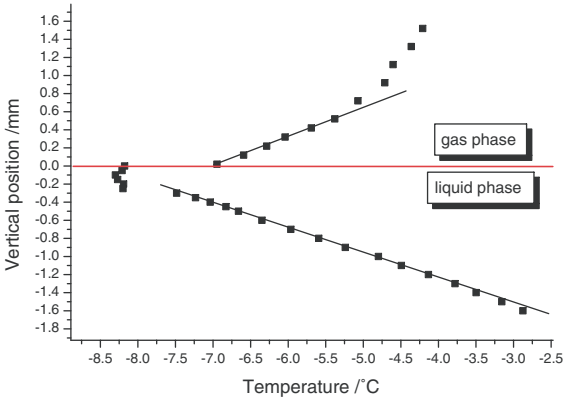

Fig. 10. Temperature profile on the centre line with evaporation (enlarged); water temperature at entry = -0.26 ± 0.07 °C.

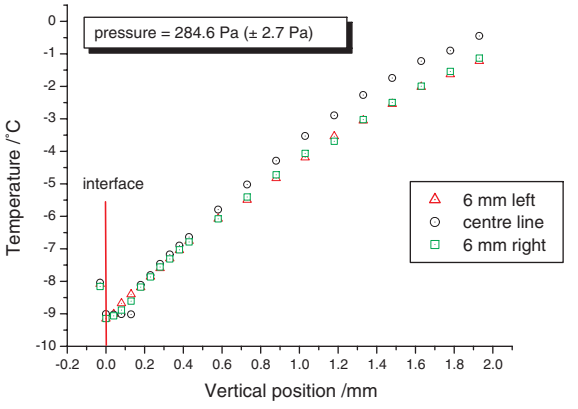

Fig. 11. Temperature profile comparison in the liquid phase, $x = -6$, 0 and +6 mm; water temperature at entry = 0.00 ± 0.05 °C, -0.21 ± 0.06 °C and $+0.05 \pm 0.05$ °C, respectively.

surface, 2.735 g cm^{-2} s^{-1}, as determined from the flow rate from the microlitre syringe, was significantly greater than from the curved surface, 1.876 g cm^{-2} s^{-1}. The corresponding temperature jumps from the liquid to the vapour phase were 1.03 °C for the flat surface and 1.53 °C for the curved surface. The lower evaporation rate can be attributed to the greater depth with the curved surface, causing a higher thermal resistance to heat transfer from the bottom of the channel to the surface and so also a larger temperature jump.

3.3. Temperature jump distribution over the whole surface, Marangoni convection

In the final set of experiments the temperature jump distribution was measured both along and transverse to the centre line to establish its dependence on the position on the surface. In Fig. 12 along the centre line (parallel to the y-axis in Fig. 1) the temperature jump distribution is approximately constant at all seven positions, confirming two-dimensionality of the temperature distribution. Transverse to the centre line (parallel to the x-axis), Fig. 13, the temperature distribution measured along the interface was symmetric with the temperature at the channel wall higher than at the centre line. A similar variation was reported for a conical cell by Ward and Duan [21]. The surface tension will vary inversely with the temperature, so that a higher surface tension will be found on the centre line of the channel. This surface tension gradient could induce thermocapillary (or Marangoni) convection from the periphery towards the centre line. Marangoni convection would be an important contributor to the energy transport because, according to the Stefan condition, energy transported by conduction only accounts for approximately 30% of the energy required to evaporate the liquid.

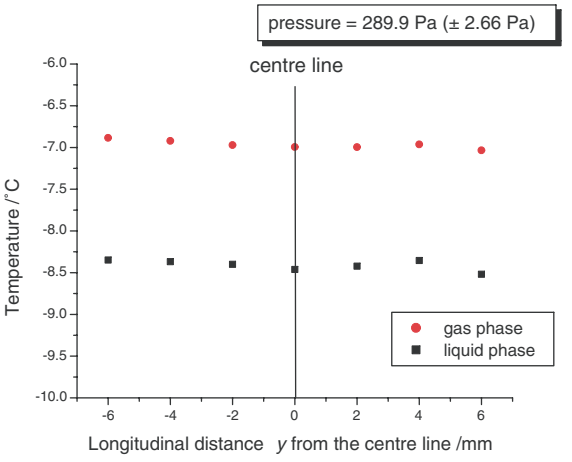

Fig. 12. Temperature jump distribution (longitudinal), water temperature at entry +0.57 ± 0.04 °C.

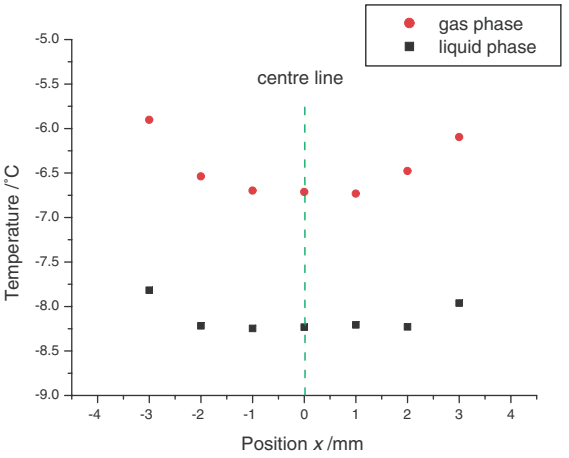

Fig. 13. Temperature jump distribution (transverse), water temperature at entry +0.63 ± 0.03 °C.

Marangoni convection also provides a possible explanation for the observed uniform temperature layer. The convecting flows along the interface coming from the walls on either side of the channel interacted on the centre line of the channel where the resulting mixing could be responsible for the uniform temperature layer.

4. Conclusions

In this paper, the design, construction and set-up of a test section for detailed studies of evaporation of liquids through free surfaces has been described. The basic ideas for such a test section were taken from the references [4,12,24], but in contrast to the axisymmetric liquid pool used there, the present test rig provided a channel-like pool of liquid; in the central part of the test section nominally two-dimensional flow, heat and mass transfer should exist.

A first set of measurements yielded temperature distributions in the liquid and vapour phases. Extrapolation of these temperatures towards the common interface showed that temperature jumps at the interface exist of the kind reported before by Ward and co-workers, with higher temperature in the vapour than in the liquid at the interface. With increased evaporation rate, i.e., with a decrease of the pressure in the vapour phase, the temperature jump at the interface increased. A uniform temperature layer just below the interface was observed; the thermal conditions were chosen so that there was no buoyancy driven convection. The measured temperature profile in the liquid bulk indicated that energy would be transported by conduction, but for the measured evaporation rate this mode of energy transport could be responsible for only a proportion of the total energy transport required to evaporate the liquid.

Consistent with the measured temperature profile along the interface, it is suggested that Marangoni convection could transport the rest of the energy and cause the observed uniform temperature layer.

Further investigation of the conditions near the interface during liquid evaporation is needed before the role of each transport mechanism can be established. The apparatus described is capable of providing information needed to gain a fuller understanding than we have at present. The two-dimensional geometry may permit the application of optical instrumentation close to the interface.

Acknowledgment

The authors are pleased to acknowledge the efforts of Dr. B. Schirmer in assembling the equipment in the early stages of the project.

References

[1] D. Bedeaux, L.J.F. Hermans, T. Ytrehus, Slow evaporation and condensation, Physica A 169 (1990) 263.
[3] J.A.W. Elliott, C.A. Ward, The statistical rate theory description of beam-dosing adsorption kinetics, J. Chem. Phys. 106 (1997) 5667.
[4] G. Fang, C.A. Ward, Temperature measured close to the interface of an evaporating liquid, Phys. Rev. E 59 (1999) 417.
[5] G. Fang, C.A. Ward, Examination of the statistical rate theory expression for liquid evaporation rates, Phys. Rev. E 59 (1999) 441.
[6] K. Hisatake, S. Tanaka, Y. Aizawa, Evaporation rate of water in a vessel, J. Appl. Phys. 73 (1993) 7395.
[7] M. Knudsen, Die maximale Verdampfungsgeschwindigkeit des Quecksilbers, Ann. Phys. Chem. 47 (1915) 697.
[8] L.D. Koffman, M.S. Plesset, L. Lees, Theory of evaporation and condensation, Phys. Fluids 27 (1984) 876.
[10] D.R. Lide, CRC Handbook of Chemistry and Physics, CRC Press LLC, Cleveland, OH, 2002.
[11] R. Marek, J. Straub, Analysis of the evaporation coefficient and the condensation coefficient of water, Int. J. Heat Mass Transfer 44 (2001) 39.
[12] A.J.H. McGaughey, C.A. Ward, Temperature discontinuity at the surface of an evaporating droplet, J. App. Phys. 91 (2002) 6406.
[13] Y.-P. Pao, Application of kinetic theory to the problem of evaporation and condensation, Phys. Fluids 14 (1971) 306.
[14] Y.-P. Pao, Temperature and density jumps in kinetic theory of gases and vapors, Phys. Fluids 14 (1971) 1340.
[15] P. Rahimi, C.A. Ward, Effect of pressure on the rate of evaporation from capillaries: statistical rate theory approach, Int. J. Heat Mass Transfer 47 (2004) 877.
[16] R.W. Schrage, A Theoretical Study of Interphase Mass Transfer, Columbia University Press, New York, 1953.
[17] P.N. Shankar, M.D. Deshpande, On the temperature distribution in liquid–vapor phase change between plane liquid surfaces, Phys. Fluids A 2 (1990) 1030.
[18] L.E. Sissom, D.R. Pitt, Elements of Transport Phenomena, McGraw-Hill, Toronto, 1972, p. 655.
[19] J. Stefan, Über die Theorie der Eisbildung, insbesondere über der Eisbildung in Polarmäre, Ann. Phys. Chem. 42 (1891) 269.
[20] C.A. Ward, Effect of concentration on the rate of chemical reactions, J. Chem. Phys. 79 (1983) 5605.
[21] C.A. Ward, F. Duan, Turbulent transition of thermocapillary flow induced by water evaporation, Phys. Rev. E 69 (2004) 056308.
[22] C.A. Ward, G. Fang, Expression for predicting liquid evaporation flux: statistical rate theory approach, Phys. Rev. E 59 (1999) 429.
[23] C.A. Ward, R.D. Findlay, M. Rizk, Statistical rate theory of interfacial transport. I. Theoretical development, J. Chem. Phys. 76 (1982) 5599.
[24] C.A. Ward, D. Stanga, Interfacial conditions during evaporation or condensation of water, Phys. Rev. E 64 (2001) 051509.